*Thermochimica Acta*, 121 (1987) 333–342
Elsevier Science Publishers B.V., Amsterdam – Printed in The Netherlands



# THERMAL POWER MEASUREMENTS IN A DIFFERENTIAL-HEAT-CONDUCTION-SCANNING CALORIMETER AT LOW TEMPERATURE-SCANNING RATES *

JORDI ORTÍN and VICENÇ TORRA

*Departament de Fisica, Universitat de les Illes Balears, 07071 Palma de Mallorca (Spain)*

HENRI TACHOIRE

*Laboratoire de Thermochimie, Université de Provence (Aix-Marseille I), 13331 Marseille Cedex 03 (France)*

(Received 1 November 1986; in final form 24 February 1987)

## ABSTRACT

The energy resolution and the ability to separate different impulsive phenomena in a heat-conduction calorimeter have been analyzed. Using a very simple model of localized constants, the experimental conditions required for a proper determination of the energy change in a first-order phase transition are obtained. In particular, the work deals with the calorimeters currently used to study the energy change and the thermal dynamics of shape-memory alloys during a martensitic transformation. These calorimeters work at low rates of temperature scanning, around 0.5 K $min^{-1}$. Our results, in addition, show how similar problems can be dealt with when operating conventional thermal analysis devices, such as DSC and DTA.

## INTRODUCTION

Heat-conduction calorimeters, using semiconductor thermobatteries as detectors, are being extensively used for the characterization of the energy change and the thermal power dynamics during the thermoelastic transformation of shape-memory alloys. The resulting calorimetric thermograms are highly sensitive to the thermo-mechanical history of the material [1–4].

These calorimeters, differential in design [5], show a very high sensitivity and are easy to operate in the range from $-180$ to $+110\,^{\circ}C$. Recently, by coupling other techniques of measurement for the electrical resistivity or the

* The authors dedicate this paper to Prof. W.W. Wendlandt on the occasion of his 60th birthday, for his numerous and relevant contributions to thermal analysis and, especially, for the effort invested in creating and promoting this journal, Thermochimica Acta, a key reference journal nowadays for all the thermoanalytical community.

0040-6031/87/$03.50 

acoustic emission (see ref. 1 and references therein), the number of possible applications has increased. It is also possible to perform, simultaneously, observations with an optical microscope [6].

In their design, the calorimeters described above present a geometry which is similar in many respects to the commercial DSC and even DTA, but they do not utilize automatic compensation. The commercial devices have been extensively studied by different groups, with the aim of better understanding the meaning of the calorimetric output, which seems to be highly influenced by the temperature programming (see, for instance, [7–16]. In fact, the problems of a commercial DSC are mainly caused by the high temperature-scanning rates at which it normally operates. The calorimeters used in this work operate at much lower rates of temperature scanning. Additionally, neither melting processes nor important changes in specific heat are involved in a martensitic transformation.

The models which have been commonly used to describe the different devices are based on heat transfer equations written for localized constants. In several cases, these models have given satisfactory pictures of the calorimetric behavior, restricted however to small temperature ranges [12,13]. As a complete martensitic transformation can easily extend over more than 30 K [3,4], our models will have to take into account any change of the parameters with temperature.

In this work, we analyze the behavior of the differential-heat-conduction-scanning-calorimeters used in thermal studies of the forward and reverse martensitic transformations occurring in shape-memory alloys. For this purpose, we draw a certain analogy between these devices and the heat-conduction calorimeters used to study liquid binary mixtures, in which the continuous injection of reactant into the vessel makes the properties of the calorimeter change slightly during the measurement [4,17,18]. We write down very simple equations for localized constants [19–23] and obtain a first approximation to the calorimetric behavior in runs with a low rate of temperature variation. The objective is to evaluate the necessary corrections for a proper determination of the energy change. In addition, we carry out first estimations of the calorimetric performances in detecting large and very fast energy dissipations, and of the way in which deconvolution should be carried out to obtain, from the thermogram, the fine thermal details of the transformation as a function of time or temperature.

## THE CALORIMETRIC SET-UP AND ITS PERFORMANCE

The basics of the experimental set-up have been extensively described elsewhere [4–6,24]. The device (Fig. 1) is formed by a calorimetric block, built in copper to improve its thermal conductivity, in which two Melcor thermobatteries are assembled differentially. Both samples, the reference

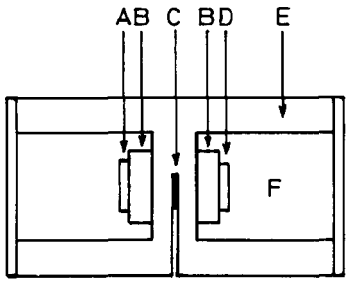


Fig. 1. Schematic drawing of an actual differential-heat-conduction-scanning calorimeter: A, reference sample; B, thermobatteries; C, temperature sensor; D, sample; E, calorimetric block (isothermal or scanned in temperature); F, chamber with additional available space.

sample and the one under test, are placed on the top flat side of the thermobatteries. The top surface of the samples is left free and can be used to place other transducers in order to perform coupled measurements. The differential output signal is converted to a digital signal by a voltmeter (resolution 100 nV) and sent to the memory of microcomputer, which finally stores the information on magnetic support for future analysis. Simultaneously, the temperature of the calorimetric block is measured by means of a platinum resistance Pt-100 and also stored by the microcomputer.

Under normal working conditions, noise in the base-line centers around $\pm 200$ nV. During the martensitic transformation of a copper-based alloy, samples with a mass of 0.5 g produce signals around 1 mV. Often, the signal-to-noise ratio has a value of 5000 (for $\beta$–$\beta'$ transformations), and on certain occasions it can reach 10000 (for $\beta$–$\gamma'$ transformations). After studying the impulse response of several similar devices, we give for the main time constant an approximate value of 10 s for samples with mass $\sim 0.5$ g and in thermal equilibrium. When this is taken into account, very fast thermal dissipations giving signals above 1 $\mu$V are clearly visible on the thermogram. In a first approximation, impulse signals close to 10 $\mu$V s can be resolved. As the sensitivity of the detectors near room temperature is approximately 400 mV $W^{-1}$, the final energy resolution of the device is 25 $\mu$J. The martensitic transformation in CuZnAl typically releases or absorbs 6 J $g^{-1}$, and consequently the calorimeter should be able, in principle, to detect instantaneous transforming portions of mass of $\sim 4$ $\mu$g.

Under the assumption that scanning the temperature at low rates does not modify the dynamic properties of the calorimeter, the thermal processes taking place in the material are detected with high accuracy in time and temperature [1,4,24]. For example, the usual scanning rates vary between 0.2 and 0.5 K $min^{-1}$. This gives, on the thermogram, the capability of distinguishing between two sudden and elementary transformations occurring with a time difference near the value of the main time constant, i.e. with a difference in temperature of only 0.05 K.

An inverse filtering of the thermogram, using two or three time constants, increases the temporal resolution by two orders of magnitude. This, in principle, gives enough resolution to separate signals to 0.001 K.

If the temperature scanning is carried out at lower or much lower rates, the resolution in temperature increases correspondingly. This will probably be inadequate when studying the transformation as a whole, as it extends often through an interval of 20 or 30 K. In the present state of the art, in fact, the required computer calculations are rarely done, and this high resolution is never achieved. This is mainly because the high resolution demands data acquisition at sampling rates around 0.05 s (20 Hz) and the storage of approximately 100,000 calorimetric samples per transformation for further analysis.

## THE TIAN EQUATION FOR A CALORIMETER WITH CHANGING TEMPERATURE

The Tian equation represents the simplest possible model of localized constants [19–23], in which only one element is considered. For a time-invariant system with $C_1$ as the heat capacity, $P_1$ as the thermal coupling to the thermostat and $W(t)$ as the thermal power released in the calorimetric cell as a function of time, and if a constant reference temperature is assumed $T_0 = 0$, the Tian equation reads

$$W(t) = C_1\left(\frac{\mathrm{d}T_1}{\mathrm{d}t}\right) + P_1T_1 \tag{1}$$

If the reference temperature is programmed as a function of time, $T_0 = T_0(t)$, the system is now a time-varying one. The temperature difference detected by the thermobatteries is $T_1 - T_0$ and the corresponding Tian equation is

$$W(t) = C_1\left(\frac{\mathrm{d}(T_1 - T_0)}{\mathrm{d}t}\right) + C_1\left(\frac{\mathrm{d}T_0}{\mathrm{d}t}\right) + P_1(T_1 - T_0) \tag{2}$$

When the temperature changes, in addition to the Newtonian term of heat flow sent to the reference block, there will be at least a progressive contribution due to radiation between the heat capacity $C_1$ of the calorimetric vessel and the surroundings. As the usual temperature programs are rather slow, the temperature differences will be very small. In this situation, for large intervals of temperature $T_0$, and as a first approximation, we can consider the thermal coupling $P_1$ to be caused by a double contribution

$$P_1 = P_{01} + P_{11}\tilde{T}^3 \tag{3}$$

where $\tilde{T}$ is an average temperature between the temperatures of the cell and of the surroundings. For the sake of simplicity, in order to proceed with the discussion, we will consider that $\tilde{T}$ and its first derivative $\mathrm{d}\tilde{T}/\mathrm{d}t$ can be approximated by $T_0$ and $\mathrm{d}T_0/\mathrm{d}t$ respectively.

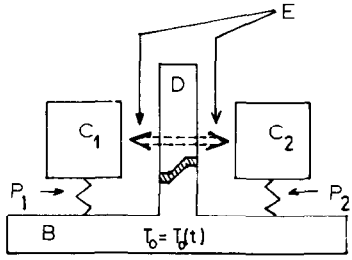


Fig. 2. Model of the heat transfer in a calorimeter following the Tian equation: B and D, calorimetric block; $C_1$ and $C_2$, heat capacities of the sample under study and of the reference sample respectively; $P_1$ and $P_2$, thermal couplings between the samples and the calorimetric block; E, direct thermal coupling between the samples.

The output electric signal of the calorimeter is caused by the Seebeck effect developed in the thermobatteries and can be taken as proportional to the absolute temperature. Therefore, in a model with a single element, the thermogram $s(t)$ will be given by

$$s(t) = A\tilde{T}(T_1 - T_0) \tag{4}$$

where the term $A\tilde{T}$ represents the Seebeck effect at a temperature $\tilde{T}$.

The Tian equation now reads

$$W(t) = C_1 \frac{d}{dt}\left(\frac{s(t)}{A\tilde{T}}\right) + C_1\left(\frac{dT_0}{dt}\right) + \left(P_{01} + P_{11}\tilde{T}^3\right)\left(\frac{s(t)}{A\tilde{T}}\right) \tag{5}$$

which can be rewritten as

$$W(t) = \frac{1}{A\tilde{T}}\left\{C_1\left(\frac{ds}{dt}\right) + \left[P_{01} + P_{11}\tilde{T}^3 - \left(\frac{C_1}{\tilde{T}}\frac{d\tilde{T}}{dt}\right)\right]s(t)\right\} + C_1\left(\frac{dT_0}{dt}\right) \tag{6}$$

Considering that the actual calorimeter is assembled differentially, we have to include a second passive element in the model (Fig. 2), with no direct thermal couplings to the first element. For this element, in which no power dissipation takes place, the balance equation reads

$$0 = C_2\left(\frac{dT_2}{dt}\right) + P_2(T_2 - T_0) \tag{7}$$

Let us consider a linear temperature program

$$T_0 = T_{0i} + \dot{T}_0 t$$

and calculate for it the output signal given by the detector in this second element, i.e. given by the reference thermobattery. We have now

$$C_2\left(\frac{dT_2}{dt}\right) + P_2T_2 = P_2T_0 = P_2\left(T_{0i} + \dot{T}_0 t\right) \tag{8}$$

Clearly $P_2 = P_2(\tilde{T})$ again. At a given temperature, and for low scanning rates, a particular solution of the differential eqn. (8) can be obtained by

choosing $T_2 = a + bt$, substituting in eqn. (8) and identifying the terms with the same power of $t$

$$C_2 b + P_2 a = P_2 T_{01} \quad \text{and} \quad P_2 b = P_2 \dot{T}_0$$

which gives

$$b = \dot{T}_0 \quad \text{and} \quad a = \left(P_2 T_{01} - C_2 \dot{T}_0\right)/P_2$$

From this result

$$T_2 - T_0 = -\left(\frac{C_2}{P_2}\right)\dot{T}_0 \tag{9}$$

This is related to the signal $s_{\text{ref}}$ given by the reference thermobattery through

$$T_2 - T_0 = \frac{s_{\text{ref}}}{\mathrm{A}\tilde{T}} = -\left(\frac{C_2}{P_2}\right)\dot{T}_0 \tag{10}$$

It is very easy to see that an equivalent result

$$T_1 - T_0 = \left(\frac{s}{\mathrm{A}\tilde{T}}\right) = -\left(\frac{C_1}{P_1}\right)\dot{T}_0 \tag{11}$$

is obtained for the first element, under the same conditions, if no thermal power is dissipated in it, i.e. if $W(t) = 0$. Therefore, we see that if $C_1 = C_2$ and $P_1 = P_2$ the differential assembly of the thermobatteries (Fig. 2) will eliminate any drift in the baseline because the same signal is produced in each thermobattery.

Writing every term in the heat balance of the second element of the model explicitly gives

$$0 = \frac{1}{\mathrm{A}\tilde{T}}\left\{C_2\left(\frac{\mathrm{d}s_{\text{ref}}}{\mathrm{d}t}\right) + \left[P_{02} + P_{12}\tilde{T}^3 - \left(\frac{C_2}{\tilde{T}}\frac{\mathrm{d}\tilde{T}}{\mathrm{d}t}\right)\right]s_{\text{ref}}(t)\right\} + C_2\left(\frac{\mathrm{d}T_0}{\mathrm{d}t}\right) \tag{12}$$

Then, if $C_1 = C_2 = C$ and $P_1 = P_2 = P$, and the balance for the second element is subtracted from the balance for the first element we get

$$W(t) = \frac{1}{\mathrm{A}\tilde{T}}\left\{C\frac{\mathrm{d}s^*}{\mathrm{d}t} + \left[P_0 + P_1\tilde{T}^3 - \left(\frac{C}{\tilde{T}}\frac{\mathrm{d}\tilde{T}}{\mathrm{d}t}\right)\right]s^*(t)\right\} \tag{13}$$

where $s^* = s(t) - s_{\text{ref}}(t)$.

Equation (13) shows the existence of a term

$$-\frac{C}{\tilde{T}}\frac{\mathrm{d}\tilde{T}}{\mathrm{d}t}$$

which will contribute positively or negatively depending on the sign of the temperature program.

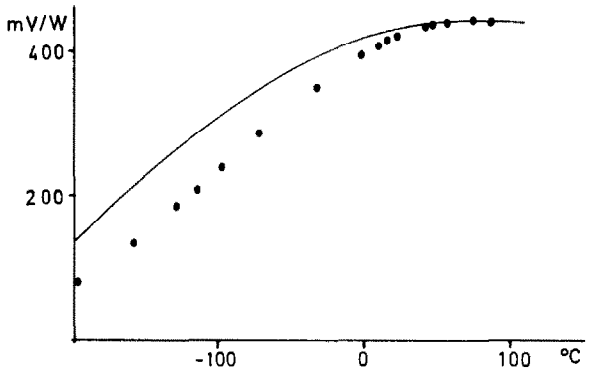


Fig. 3. Sensitivity (mV $W^{-1}$) vs. temperature (°C): ●, experimental values from a typical calorimeter; ———, sensitivity of a model with coupling accounting for radiation.

In addition, the procedure followed to obtain eqn. (13) shows that any difference in the thermal properties of one element with respect to the other will result in extra dissipations. They have, for example, the form

$$(C_1 - C_2)\left(\frac{dT_0}{dt}\right)$$

and are increasingly important for increasing temperature rates.

The following is restricted to a perfectly differential situation and studies the way in which the temperature program affects the sensitivity of the calorimeter. First, consider the static sensitivity, i.e. the sensitivity determined at a constant temperature $\tilde{T}$ from standard calibrations using a Heaviside-like input power released by means of the Joule effect. With $d\tilde{T}/dt = 0$, and $ds^*/dt = 0$, once the steady state has been reached, we obtain from eqn. (13)

$$S(\tilde{T}) = \frac{s^*(\text{Heaviside})}{W} = \frac{A\tilde{T}}{P_0 + P_1\tilde{T}^3} \tag{14}$$

Figure 3 shows several values of the static sensitivity at different temperatures, experimentally determined using the Joule effect, compared with the behavior predicted by the model. The qualitative agreement is to be emphasized, in light of the crude description given by the model and the approximations that we have been using.

The dynamic sensitivity $S_{dyn}$ is the sensitivity of the calorimeter when the temperature of the block increases or decreases with time following a predetermined temperature program. The value of $S_{dyn}$ can be obtained from the model by simply considering a permanent output signal as the response to a constant input power, i.e. $ds^*/dt = 0$. The result is

$$S_{dyn}(\tilde{T}) = \frac{s^*(\text{Heaviside})}{W} = \frac{A\tilde{T}}{P_0 + P_1\tilde{T}^3 - \left(\frac{C}{\tilde{T}}\frac{d\tilde{T}}{dt}\right)} \tag{15}$$

The dynamic sensitivity is therefore dependent on the rate of temperature change and the contribution changes its sign depending on whether the calorimeter is being cooled or heated. If $d\tilde{T}/dt > 0$ then $S_{dyn}(\tilde{T}) > S(\tilde{T})$; if $d\tilde{T}/dt < 0$ then $S_{dyn}(\tilde{T}) < S(\tilde{T})$.

There is, however, a partial compensation to this effect. The geometry of the calorimeter causes the calorimetric block to be the element in greater contact with the external surroundings, which drive the temperature program. Consequently the block will have a slightly higher temperature than the rest of the calorimeter on heating, and a slightly lower temperature than the rest of the calorimeter on cooling. This means that $S_{dyn}$ will be larger (smaller) than the static sensitivity $S$, but the temperature $\tilde{T}$ measured in the block will also be higher (lower) than the actual temperature inside the calorimeter. These effects tend to compensate each other, giving dynamic sensitivities very similar to the static ones at corresponding temperatures.

To obtain the total energy involved in a transformation we integrate the thermal power $W(t)$ given by eqn. (13) from the time $t_1$ at which the process begins until the time $t_2$ at which it ends.

$$\int_{t_1}^{t_2} W\,dt = \int_{t_1}^{t_2} C\frac{d}{dt}\left(\frac{s^*}{A\tilde{T}}\right)dt + \int_{t_1}^{t_2} P\left(\frac{s^*}{A\tilde{T}}\right)dt$$

$$= 0 + \int_{t_1}^{t_2}\left(P_0 + P_1\tilde{T}^3\right)\left(\frac{s^*}{A\tilde{T}}\right)dt = \int_{t_1}^{t_2}\left(\frac{s^*}{S(\tilde{T})}\right)dt \qquad (16)$$

It is clear that the utilization of the static sensitivity gives the correct result, but only if there are not important changes in the specific heat capacity $C$ during the process.

Finally, we analyze the effect of the temperature variation on the dynamic response of the calorimeter and sketch, from the analysis, the way in which a proper deconvolution of the thermogram should be carried out in order to recover, as exactly as possible, the thermal power dissipated by the process as a function of time or temperature. This is a much more difficult problem, and the differential version of the Tian equation that we have been using to simulate the behavior of the calorimeter is not detailed enough to afford it. To see this, consider the main time constant of the model, as deduced from eqn. (13)

$$\tau_1 = \frac{C}{P_0 + P_1\tilde{T}^3 - \left(\frac{C}{\tilde{T}}\frac{d\tilde{T}}{dt}\right)} \qquad (17)$$

In spite of the poor accuracy with which the time constants are determined experimentally, the actual changes of $\tau_1$ (see ref. 4) are never as important as those predicted by eqn. (17).

As the total energy is the integral of the thermogram, the description of the energy calculations given by the model is qualitatively correct. However,

a first analysis of the deconvolution problem shows that more elaborate models will have to be developed to deal with it. As a first approximation an inverse filtering, with parameters (poles and zeros) varying with temperature just as the parameters isothermally determined do, seems to be reasonable. Since the impulse response of the calorimeter vanishes after 50 or 60 s, the dynamic properties of the calorimeter at a given temperature, when scanning the temperature at rates of the order of 0.3 K $min^{-1}$, have to be largely determined by the dynamic properties of the calorimeter working isothermally at the given temperature. Other changes in the dynamic properties [4] can arise from important local changes in the transforming material occurring in burst-like transformations ($\beta$–$\gamma'$).

The modeling of standard commercial devices (DSC or DTA) is far more difficult: not only have the conditions $C_1 = C_2$ and $P_1 = P_2$ to be fulfilled, but often there is a direct variable thermal coupling between elements 1 and 2 [7,11–13], as represented by the arrow E in Fig. 2. During a calorimetric run, important changes in the heat capacity $C_1$ and in the thermal coupling between the sample and the cell containing the sample may also occur. The higher the rate of scanning the temperature, the more difficult it is to evaluate all these contributions in order to sketch a calorimetric model.

## CONCLUSIONS

(1) The energy resolution of the differential-heat-conduction-scanning calorimeters, which are being used to study the martensitic transformation undergone by shape-memory alloys, centers around 25 $\mu$J for a nearly-instantaneous transformation in part of the material. For the CuZnAl alloys this represents a simultaneous transforming mass of the order of 4 $\mu$g. For low rates of scanning in temperature, 0.3 K $min^{-1}$ on average, a proper inverse filtering of the thermogram produces a corrected signal in which it is possible to distinguish between thermal effects with a difference in temperature of only 0.001 K.

(2) The total energy released or absorbed in a transformation can be obtained accurately from the experimental thermogram under certain conditions. First, the calorimeter should be calibrated, determining the sensitivity under isothermal conditions at different temperatures in the range $-180$ to $+110\,^{\circ}C$. If the heat capacities of both sample and reference are equal, and the configuration is symmetrical for them, the energy of the transformation can be easily calculated from the thermogram and the sensitivity obtained isothermally.

## ACKNOWLEDGMENT

Financial support of this work by the CAICyT (Spain) within the Research Project 3562-83 is gratefully acknowledged.

REFERENCES


1 H. Tachoire, J.L. Macqueron and V. Torra, in M.A.V. Ribeiro da Silva (Ed.), Thermochemistry and its Applications to Chemical and Biochemical Systems, Reidel, Dordrecht, 1984, pp. 77–126.
2 M. Mantel, Influence de l'ordre atomique et des défauts ponctuel sur la stabilisation de la phase martensitique dans un aliage à mémoir de forme CuZnAl, Thesis, INSA-Lyon, 1985.
3 C. Picornell, C. Seguí, V. Torra, C. Auguet, Ll. Mañosa, E. Cesari and R. Rapacioli, Thermochim. Acta, 106 (1986) 209.
4 H. Tachoire, J.L. Macqueron and V. Torra, Thermochim. Acta, 105 (1986) 333.
5 A. Gery, G. Sinicki, M. Laurent and J.L. Macqueron, C.R. Acad. Sci. Paris, B, 266 (1968) 113.
6 V. Torra, J.M. Guilemany and E. Cesari, Thermochim. Acta, 99 (1986) 19.
7 W.W. Wendlandt, Thermal Methods of Analysis, Wiley Interscience, New York, 1974.
8 V. Perez Villar, An. Fis., 69 (1973) 387.
9 A. Marini, V. Berbenni, V. Massarotti, G. Flor and G. Campari-Vigano, Thermochim. Acta, 85 (1985) 279.
10 A. Marini, V. Berbenni, G. Flor, V. Massarotti and G. Campari-Vigano, Thermochim. Acta, 95 (1985) 419.
11 P. Claudy, J.C. Commercon and J.M. Letoffe, Thermochim. Acta, 65 (1983) 245.
12 P. Claudy, J.C. Commercon and J.M. Letoffe, Thermochim. Acta, 68 (1983) 305.
13 P. Claudy, J.C. Commercon and J.M. Letoffe, Thermochim. Acta, 68 (1983) 317.
14 J. Reichelt and W. Hemminger, Thermochim. Acta, 69 (1983) 59.
15 G.W.H. Höhne, Thermochim. Acta, 69 (1983) 175.
16 W. Hemminger and G. Höhne, Calorimetry, Verlag Chemie, Weinheim, F.R.G., 1984.
17 J. Ortín, A. Ramos and V. Torra, Thermochim. Acta, 84 (1985) 255.
18 J. Ortín, C. Rey and V. Torra, Thermochim. Acta, 96 (1985) 37.
19 W. Zielenkiewicz and E. Margas, Bull. Acad. Polon. Sci., Ser. Sci. Chim., 16 (1968) 101; and 16 (1968) 133.
20 K.L. Churney, E.D. West and G.T. Armstrong, A cell model for isoberibol calorimeters, NBSIR 73-184, Washington D.C.
21 J.L. Macqueron, J. Navarro and V. Torra, An. Fis., 73 (1977) 163.
22 A. Isalgué, J. Ortín, V. Torra and J. Viñals, An. Fis., 76 (1980) 192.
23 J. Navarro, E. Cesari, V. Torra, J.L. Macqueron, J.P. Dubes and H. Tachoire, Thermochim. Acta, 52 (1982) 175.
24 C. Picornell, C. Seguí, V. Torra, J. Hernáez and C. López del Castillo, Thermochim. Acta, 91 (1985) 311.